Thin-film thickness profile measurement by three-wavelength interference color analysis

Katsuichi Kitagawa

Toray Engineering Co. Ltd., 1-1-45 Oe, Otsu 520-2141, Japan (katsuichi_kitagawa@toray-eng.co.jp)

Conventional transparent film thickness measurement methods such as spectroscopy are essentially capable of measuring only a single point at a time, and their spatial resolution is limited. We propose a film thickness measurement method that is an extension of the global model-fitting algorithm developed for three-wavelength interferometric surface profiling. It estimates the film thickness distribution from an interference color image captured by a color camera with three-wavelength illumination. The proposed method is validated through computer simulations and experiments.   © 2013 Optical Society of America

OCIS codes: 120.3180, 120.3940, 240.0310, 310.6860.

1. Introduction

Conventional transparent film thickness measurement techniques, such as spectroscopy and ellipsometry, generally adopt a single-point measuring method, resulting in long measurement times for thickness mapping. Another drawback of these techniques is their low spatial resolution. To overcome these problems, researchers have developed various two-dimensional (2D) measurement techniques that can measure film thickness using a TV camera. Some typical examples of such techniques are imaging spectrophotometry [1,2] and ellipsometric imaging [3,4]. However, these techniques either require the use of an expensive camera or involve a complex procedure.

Another approach for measuring film thickness is to determine the interference color. The interference color phenomenon of thin films is seen in soap bubbles, and the relationship between the color and the thickness of a film has been investigated for many years and is represented in the Newton color chart. The knowledge of this relationship has been used for measuring semiconductor film thickness [5,6], the flying height of magnetic heads [7], and lubricant film thickness [8,9]. A typical example is the lubricant film thickness measurement system described by Eguchi and Yamamoto [9], in which a color camera captures the interference image, and the film thickness at each pixel is estimated from its hue by using the calibration data obtained in advance.

However, techniques based on the use of the interference color have rarely been used in the industry. The most serious problem with them is that they require frequent calibration because the color–thickness relationship depends on a variety of environmental conditions, such as illumination and target film structure. Another problem with them is their narrow unambiguous measurement range of a few hundred nanometers, resulting from the cyclic repetition of colors depending on thickness.

To overcome these problems, we propose a 2D film thickness measurement method, named global model fitting for thickness (GMFT), which is an extension of the global model-fitting algorithm developed for three-wavelength interferometric surface profiling [10,11]. We validate the proposed method using both simulations and experiments.
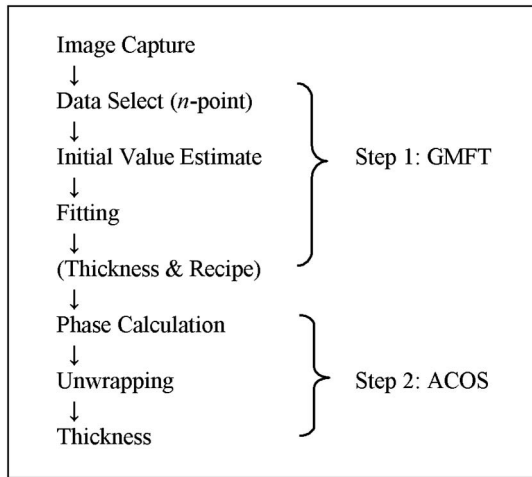
Fig. 1. Flowchart of the proposed algorithm.

Fig. 2. (Color online) BGR intensities and synthesized color chart as a function of film thickness.

2. Principle of the GMFT Method

Our algorithm consists of two steps, and its flowchart is shown in Fig. 1. Step 1 consists of the GMFT method, which is used to estimate the thickness of each pixel from its color information. Because of the high computational cost, this method is applied to a limited number of pixels during actual use. Step 2 consists of another method, named the arccosine (ACOS) method, which calculates the thickness of the other pixels within a shorter period of time, by using the information obtained from step 1. This information is also applicable to other images captured under the same optical conditions. For this reason, it can be referred to as a "recipe."

A. GMFT Method

1. Relationship Between Color and Thickness

Consider light incident on a thin film and reflected by both the upper and lower boundaries. After ignoring multiple reflections, we can obtain the following intensity of the sum of the two reflected waves:

$$I(\lambda) = I_1(\lambda) + I_2(\lambda) + 2\sqrt{I_1(\lambda)I_2(\lambda)}\cos\{\delta(\lambda)\}, \quad (1)$$

where I_1 and I_2 are the intensities of the waves, λ is the wavelength, and δ is the phase difference between them. Assuming a uniform refractive index, $n(\lambda)$, and normal incidence of light, the optical path difference (OPD) between the two reflections from a thin film is $\mathrm{OPD} = 2n(\lambda)t$, where t is the thickness of the layer. Therefore the phase difference for light reflected from the two surfaces is $\delta(\lambda) = 2\pi\,\mathrm{OPD}/\lambda = 4\pi n(\lambda)t/\lambda$. For a nondispersive medium (i.e., $n(\lambda) = n$), we obtain

$$I(\lambda) = I_1(\lambda) + I_2(\lambda) + 2\sqrt{I_1(\lambda)I_2(\lambda)}\cos(4\pi nt/\lambda). \quad (2)$$

Let us consider a case of three-wavelength (B, G, R) illumination. By assuming that $I_1 = I_2 = 1/2$, $\lambda_B = 470$ nm, $\lambda_G = 560$ nm, and $\lambda_R = 600$ nm, we calculated the theoretical intensities of each wavelength
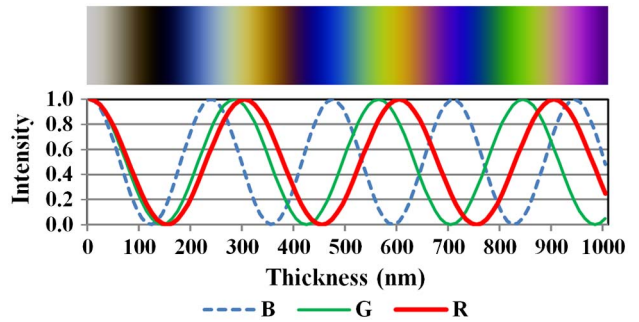
for the optical thickness range 0–1000 nm and then obtained the synthesized color chart. The results are shown in Fig. 2. It should be noted that the color change is due to the cyclic variation in BGR signals according to the film thickness. This means that we can estimate the film thickness from the BGR signals, instead of from the color information.

Three-wavelength BGR signals can be obtained by an interference color imaging system, which is shown in Fig. 3. This is almost the same configuration as that of the three-wavelength single-shot interferometry reported by Kitagawa [12]. The details of the actual apparatus are discussed later in Section 4.

2. GMFT Algorithm

Although the case of three wavelengths was considered in Fig. 2, in the following equations, we assume a more generalized expression for m wavelengths.

When we capture interference images of m wavelengths, the observed intensity $g(i,j)$ at the point i $(i = 1, 2, ..., n)$ and for wavelength j $(j = 1, 2, ..., m)$ is given by the following model:

$$g(i,j) = a(j)[1 + b(j)\cos\{\phi(i,j)\}], \quad (3)$$

where $a(j)$ and $b(j)$ are the DC bias and the modulation of the waveform, respectively, and $\phi(i,j)$ is the phase given by
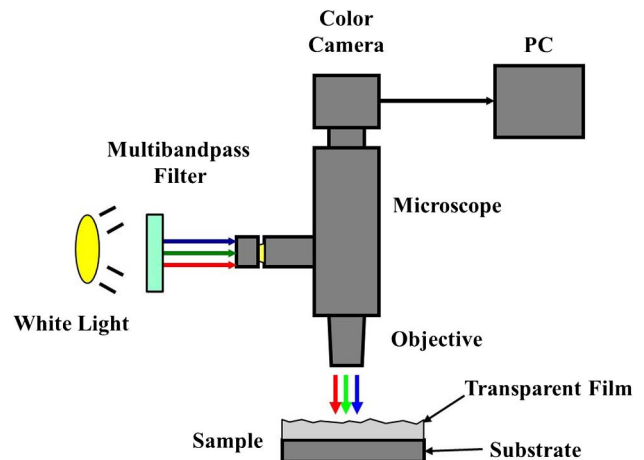

Fig. 3. (Color online) Optical setup for three-wavelength interference color imaging.

$$\phi(i,j) = 4\pi n t(i)/\lambda_j, \qquad (4)$$

where n is the known refractive index, $t(i)$ is the thickness, and λ_j is the wavelength of the jth wavelength. Inserting Eq. (4) into Eq. (3) gives the following model:

$$g(i,j) = a(j)[1 + b(j)\cos\{4\pi n t(i)/\lambda(j)\}]. \qquad (5)$$

This model is derived under the assumption that the waveform parameters $a(j)$ and $b(j)$ are constant in the field of view and dependent only on the wavelength. This assumption is almost always valid when the target surface is homogeneous.

The unknown parameters $a(j)$, $b(j)$, and $t(i)$ can be estimated using the following least-squares fitting equation:

$$J[a(j), b(j), t(i)] = \sum_{i=1}^{n} \sum_{j=1}^{m} [g(i,j) - g_{ij}]^2, \qquad (6)$$

where $g(i,j)$ is the model intensity defined by Eq. (5) and g_{ij} is the observed intensity.

This nonlinear least-squares problem can be solved by many numerical methods. In this paper, we used the Solver program in MS Excel for the computer simulation. For the actual experiments, we used our own program based on the Davidon–Fletcher–Powell algorithm [13].

3. Necessary Conditions
Let us consider the necessary conditions to obtain the unknown parameters $a(j)$, $b(j)$, and $t(i)$. When the number of wavelengths is m and the number of points is n, the total number of unknown parameters is $2m + n$. Since m values are observed at one point, the necessary condition for the solution is $mn \geq 2m + n$. Then, the number of points must be

$$n \geq 2m/(m-1). \qquad (7)$$

This means that $n \geq 4$ in the case of $m = 2$ and $n \geq 3$ in the case of $m = 3$. When $n = 2m/(m-1)$, then the problem becomes a $(2m + n)$-order nonlinear simultaneous equation, and when $n > 2m/(m-1)$, then the problem becomes a $(2m + n)$-order nonlinear least-squares problem.

Figure 4 illustrates the principle of this algorithm in the case of three wavelengths and n-points. From $3n$ observed intensities, we can estimate $(n + 6)$ unknown parameters, that is, n-point thicknesses and six waveform parameters.

It should be noted that to avoid the problem from becoming ill-conditioned and to obtain a good estimation, it is advisable to select the points such that their thickness distribution becomes wide.
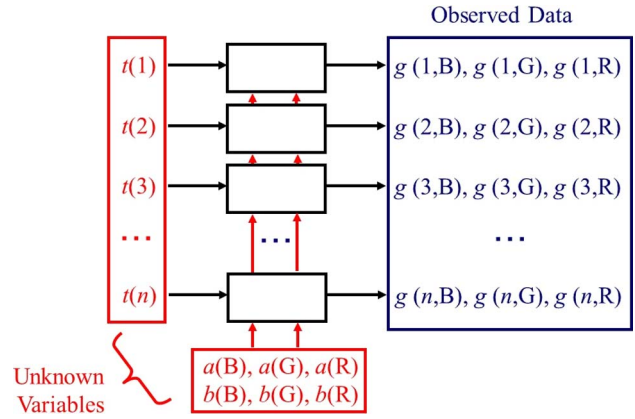

Fig. 4. (Color online) Principle of the GMFT method in the case of three wavelengths and n-point fitting.

4. Initial Estimates
To find solutions to the nonlinear least-squares problem described in the previous subsection, we use an iterative technique, which requires initial estimates that allow us to search for the minimum. Since the model function of Eq. (5) contains a cosine function, the error function has many local minima. Therefore, it is essential to make good initial estimates.

In this paper, $a(j)$ is set to be the average of the observed values, and the modulation $b(j)$ is set to be the range of the observed values (that is, the difference between the maximum and minimum observed values) divided by $2a(j)$. The thickness, $t(i)$, is a rough estimate, which is generally given by *a priori* knowledge of the target sample.

B. ACOS Algorithm
The computational cost of the nonlinear least-squares problem is very high. Hence, the method becomes impractical when the number of points is large. Therefore, we use the GMFT algorithm with a small number of points (e.g., less than 100), and then the thicknesses of the other points are calculated by the following method, named the ACOS method, which uses the estimated waveform parameters from the first step.

1. Phase Estimation
When the waveform parameters are given, the phase is obtained from the observed intensity by the following equation derived from Eq. (3):

$$\phi(i,j) = \cos^{-1}[\{g_{ij}/a(j) - 1\}/b(j)], \qquad (8)$$

where $\cos^{-1}$ is the arccosine function and its value is in the range $[0, \pi]$. When the argument of the function is not within the domain $[-1, 1]$, the function is undefined. In this case, the argument is approximated as -1 or 1.

2. Phase Unwrapping
From the phase data, the thickness, $t(i,j)$, is obtained by

$$t(i,j) = (1/n)[\pm\phi(i,j)/2\pi + N(i,j)](\lambda_j/2), \quad (9)$$

where $N(i,j)$ is the fringe order (integer), which is estimated by the coincidence method. The principle of this method is the same as the so-called exact fractions method [14] used for gauge block length measurement by multiwavelength interferometry.

Figure 5 shows an experimental example of the use of this method. For each wavelength, the thicknesses with different orders are plotted. The unknown orders are determined so that the three candidate thicknesses match best. In this case, the thickness is estimated to be 510 nm. It should be noted that the phase is obtained by the arccosine function, not by the arctangent function. Therefore, there are two candidate thicknesses for each fringe order, as shown in Fig. 5.

3. Computer Simulations

A. Test Method
A three-wavelength interference color image was synthesized with the following conditions: (a) image size = 50 × 50 pixels; (b) pixel size = 1 μm; (c) wavelengths = 470, 560, and 600 nm; and (d) target surface = sphere with 1 mm radius, with a small square protrusion of thickness 50 nm and size 4 × 4 pixels; and (e) waveform parameters of $a = 100$ and $b = 1$. The target thickness profile is shown in Fig. 6, and the synthesized image is shown in Fig. 7. It should be noted that all the thicknesses in this section are expressed in optical thickness units.

All the computations were done in MS Excel with a Windows PC. The nonlinear least-squares fitting in the GMFT method was carried out by the Solver program in MS Excel.

We performed two simulations The first one used three points for fitting, and the second one used 50 points. The coordinates of the sampled points were (5, 25), (15, 25), and (25, 25) in the first test and (1, 25), (2, 25),…, (50, 25) in the second test.
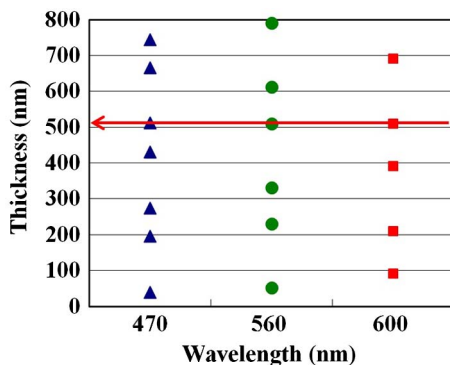

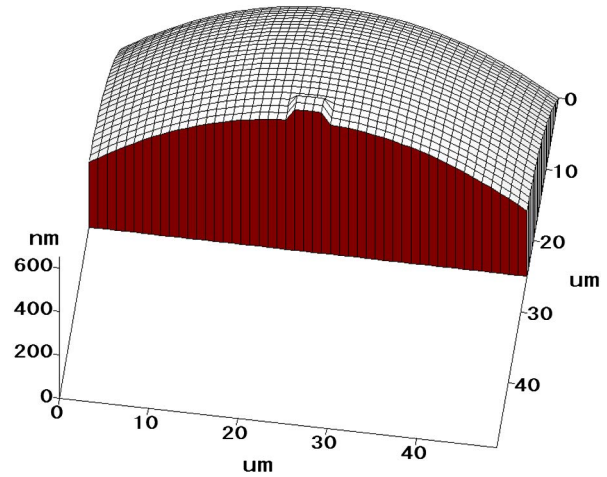Fig. 5. (Color online) Phase unwrapping by the coincidence method.

Fig. 6. (Color online) Cross section of the target thickness profile used for the simulations.

B. Test Results

1. Three-Point Fitting
The BGR images are shown in Fig. 8 with three points used for fitting. The intensity values are shown in Fig. 9. The initial estimates of the thicknesses were set at 95% of the true values. The estimated thicknesses are shown in Fig. 10 with the initial and true values. Detailed results are shown in Table 1. The parameters and thicknesses were correctly estimated using this technique.

2. 50-Point Fitting
We estimated the thickness profile of 50 points along the line $y = 25$ using 50 points for GMFT fitting. The intensities are shown in Fig. 11. The initial estimates were set to be the true thicknesses minus 50 nm. The thicknesses were estimated correctly, as shown in Fig. 12. It should be noted that the small protrusion of size 4 × 4 pixels is measured correctly without any loss in spatial resolution.

3. Thickness Estimation by the ACOS Method
Next, we estimated the thickness profile of 50 points along the line $y = 25$ using the recipe obtained by the GMFT three-point fitting. From the intensities shown in Fig. 11, the phases were obtained as shown in Fig. 13. Then, the thicknesses were estimated correctly, as shown in Fig. 14.
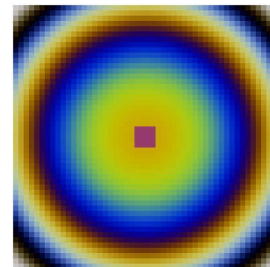

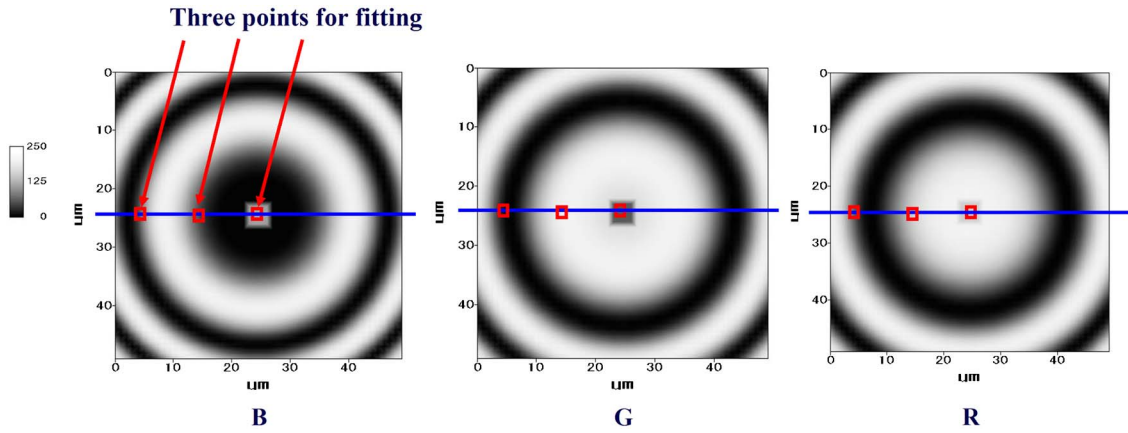Fig. 7. (Color online) Synthesized color image.

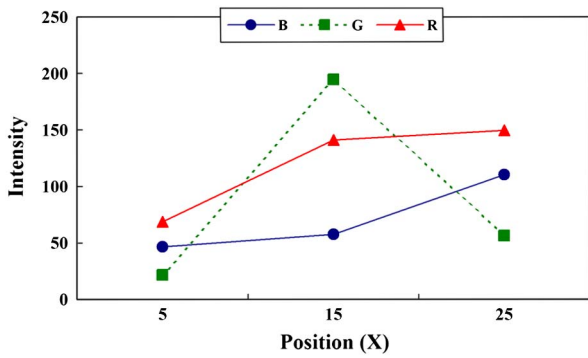Fig. 8. (Color online) BGR images and the three points used for fitting.

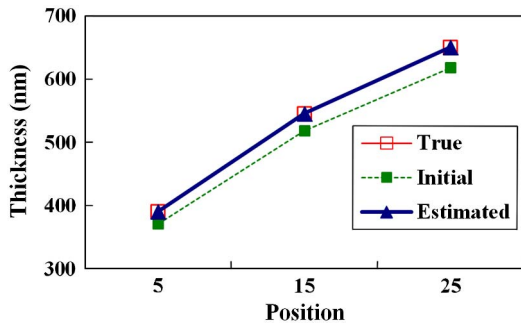Fig. 9. (Color online) Observed intensities for three-point fitting.
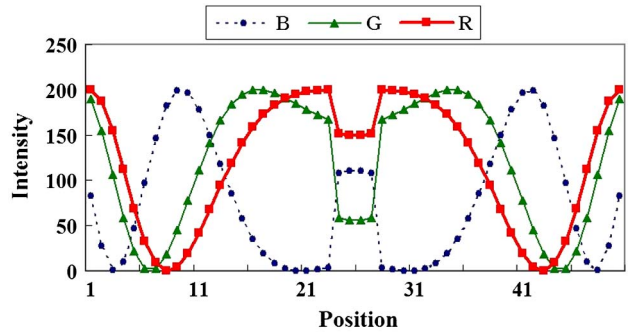

Fig. 11. (Color online) Intensity profiles for 50-point sets.

Fig. 10. (Color online) Estimated thicknesses from three-point fitting.
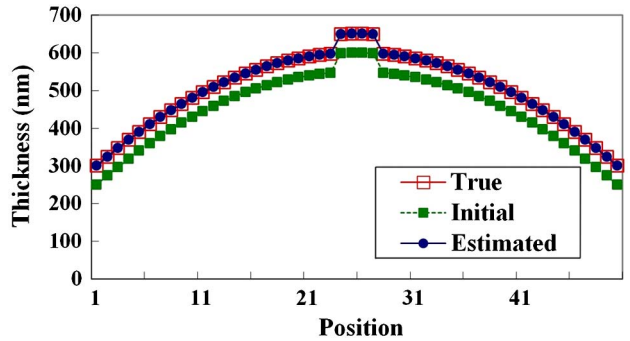
Fig. 12. (Color online) Estimated thicknesses obtained with 50-point fitting.

Table 1. Estimated Variable Values Obtained with Three-Point Fitting

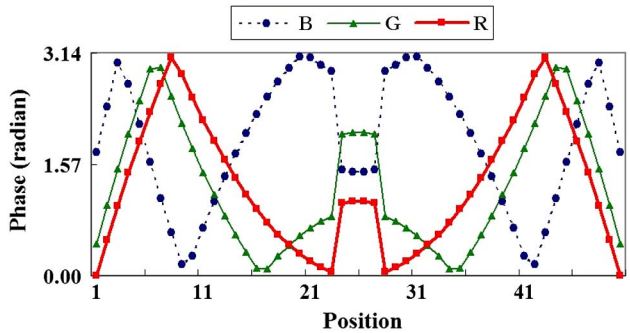| Variables		True	Initial	Estimated	Error(%)
t	$t(1)$	390	371	390	0.00
	$t(2)$	545	518	545	0.00
	$t(3)$	650	618	650	0.00
a	B	100	79	100	0.00
	G	100	108	100	0.00
	R	100	109	100	0.00
b	B	1.00	0.41	1.00	0.00
	G	1.00	0.80	1.00	0.00
	R	1.00	0.37	1.00	0.00

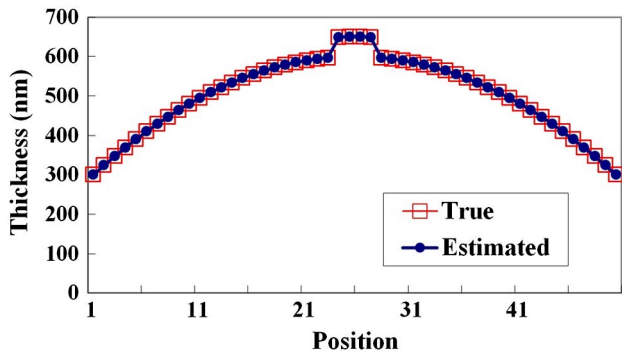Fig. 13. (Color online) Phase profiles calculated by the ACOS method.

Fig. 14. (Color online) Estimated thicknesses of 50 points obtained with the ACOS method with the recipe obtained with GMFT three-point fitting.

4. Experiments

A. Test Method

The experimental apparatus is shown in Fig. 15. The illumination unit consists of a halogen lamp and a multibandpass filter, as shown in Fig. 3. The spectral transmittance of the filter is shown in Fig. 16. The central wavelengths were 470, 560, and 600 nm, and each of their bandwidths was 10 nm. The camera was a three-CCD color camera (Hitachi, HV-F22CL) with 1360 × 1024 pixels. Its spectral sensitivity is shown in Fig. 17 for the wavelengths of the illumination. The captured image was stored in a PC memory as a raster image with a color depth of 24 bits per pixel. The color crosstalk was compensated by the crosstalk compensation algorithm reported in [11]. We wrote a program in the C language to implement the GMFT algorithm on a Windows PC.

In our experiments, a calibrated step wafer (Mikropack, Germany) was used, which consists of a 100 mm Si wafer with six silicon dioxide (SiO_2; $n = 1.46$) steps between 0 and 500 nm, as shown in Fig. 18. The captured microscopic images of the six step areas were stitched together to obtain the composite image shown in Fig. 19.

The nonlinear least-squares equation in the GMFT algorithm was solved using the Davidon–Fletcher–Powell method [13]. There were six data points to
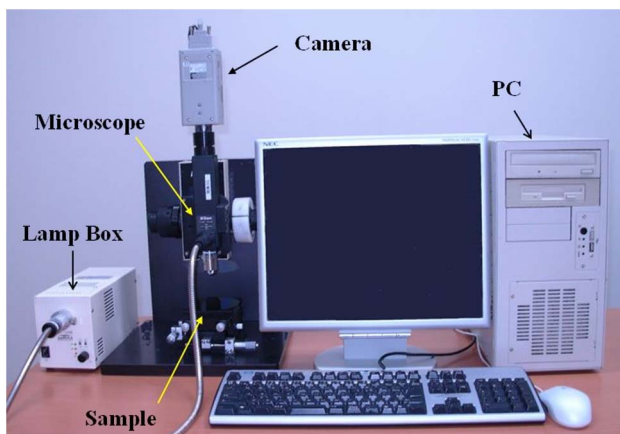

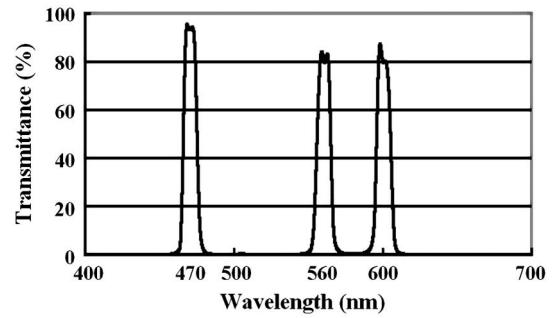Fig. 15. (Color online) Experimental apparatus.

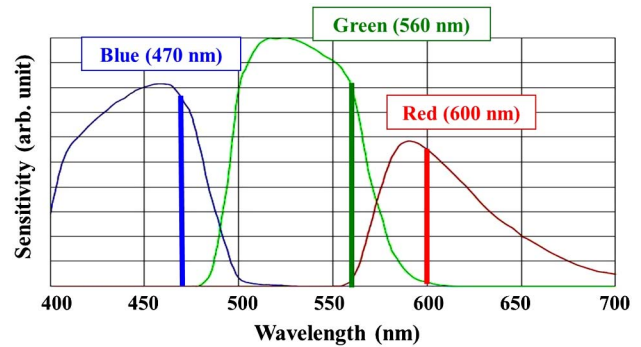Fig. 16. Spectral transmittance of the multibandpass filter.

Fig. 17. (Color online) Sensitivity of the three CCDs of the color camera. The wavelengths used in the experiment are indicated.

be fitted, each at the center of one of the step areas, as shown in Fig. 19. The initial thickness values were set to be the nominal values. The thickness range of each point was set to be the nominal value, ±50 nm.

In the second step, we calculated the thickness distribution over the whole 1344 × 1024 pixel area by using the parameters obtained in the first step.

B. Test Results

From the six-point intensity data, the corresponding thicknesses were estimated by the GMFT method. The results are shown in Table 2. Figure 20 shows a good correlation between the nominal and measured thicknesses.

Then, the thickness distribution of the whole area was measured by the ACOS method. As shown in Fig. 21, good agreement between the measured and predicted thickness distributions was obtained.

The total calculation time for 1344 × 1024 pixels was about 1.2 s, including 6 ms of GMFT fitting using a C language program running on a Windows PC
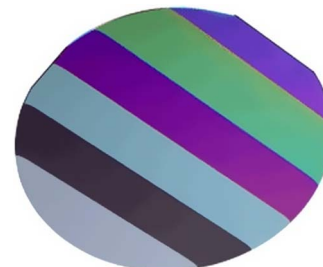

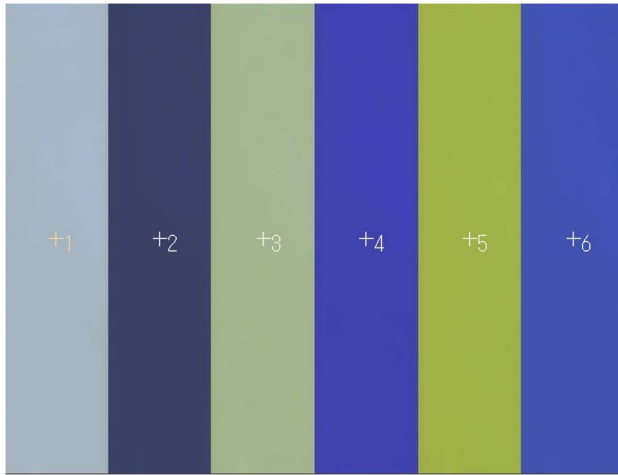Fig. 18. (Color online) Target thickness standard.

Fig. 19. (Color online) Stitched color image of thickness standard, and six points for GMFT fitting (shown in white numbers).

Table 2. Results of GMFT Fitting

Variables		Initial	Estimated
t	$t(1)$	0	0
	$t(2)$	100	107
	$t(3)$	200	197
	$t(4)$	300	300
	$t(5)$	400	396
	$t(6)$	500	504
a	B	144	133
	G	125	122
	R	113	113
b	B	0.43	0.47
	G	0.47	0.49
	R	0.47	0.46

(3.4 GHz Intel Core i7-2600 CPU). Because the calculation of the ACOS method is pixel-independent, the speed would be very much improved by a parallel processing technique.
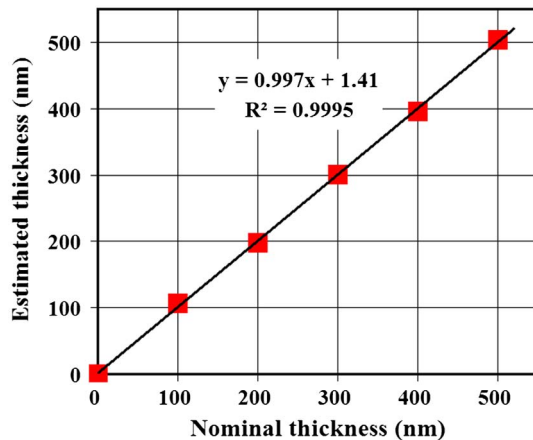

Fig. 20. (Color online) Estimated thicknesses of six points obtained using GMFT fitting.
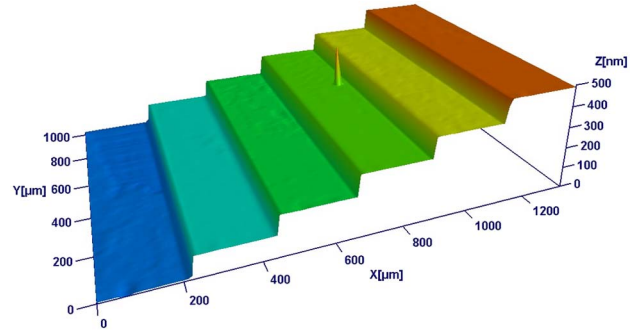

Fig. 21. (Color online) Estimated thickness profile by the ACOS method.

5. Modified Algorithms

For the practical application of the proposed method, several problems must be solved. In this section, we focus on the improvements of the algorithm.

A. Local Minima Problem

As mentioned in Subsection 2.A.4, the error function has many local minima. Therefore, it is necessary to start with the best initial estimates possible for the parameters to avoid getting trapped in local minima. In our previous study [11], we investigated the problem of how accurately the initial thicknesses must be estimated to get the true solution. Under some assumptions, the relationship between the thickness error and the sum of squared errors (SSE) was theoretically obtained, as shown in Fig. 22, and we concluded that the initial estimate of the optical thickness must be within ±80 nm of the true value.

This local minima problem can be avoided by using a global optimization algorithm. We adopted the multistart method, in which a series of starting points are selected within the defined lower and upper bounds. To validate this multistart method, we performed the same GMFT test as in Subsection 4.A —this time, with an initial thickness of 300 nm and a range of 0–550 nm. The results in Fig. 23 show the effectiveness of the global optimization method. Even with the maximum initial error of 300 nm, the correct solution is acquired. The required calculation time for this method is dependent on the number of multistarts. In the above experiments, it was $4^6 = 4096$, since the step of the multistart
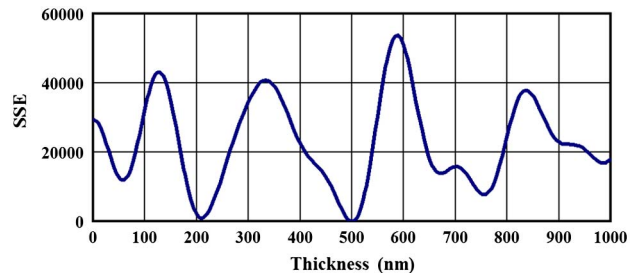

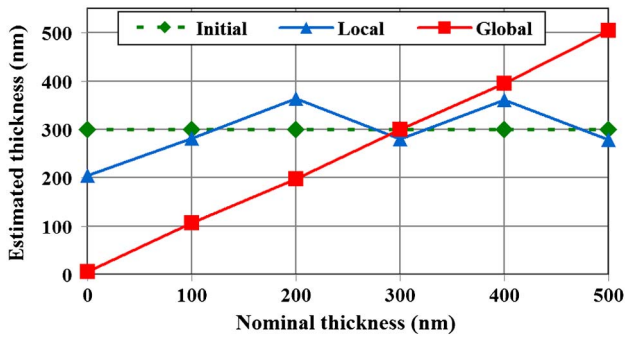Fig. 22. (Color online) SSE versus thickness error.

Fig. 23. (Color online) Estimated thicknesses by two GMFT fitting algorithms, i.e., local and global optimization methods, all with initial thicknesses of 300 nm.

method was set to 150 nm, and the time was 16 s using the Windows PC (3.4 GHz CPU).

B. Ill-Conditioned Problem

In practical applications, it is sometimes difficult to satisfy the necessary condition of the GMFT method that the number of different thicknesses must be more than three. The typical case is when the target thickness is almost uniform. Although we can easily avoid this situation in the GMF surface profiling by tilting the target surface, it is useless in the GMFT thickness profiling. To solve this problem, we have developed a modified GMFT algorithm for one-point fitting (which we call the GMFT-1 algorithm).

C. Modified GMFT Algorithm (GMFT-1)

Since there is only one unique thickness, the number of observed data is three. Therefore, only three unknown variables are acceptable. To reduce the number of unknowns, we make two assumptions. We first assume that the ratios among the bias parameters $a(j)$ are constant. Then, $a(B)$ and $a(G)$ are expressed as

Fig. 24. (Color online) Color image of the 300 nm thickness standard, and the point used for GMFT-1 fitting (indicated by the white number).
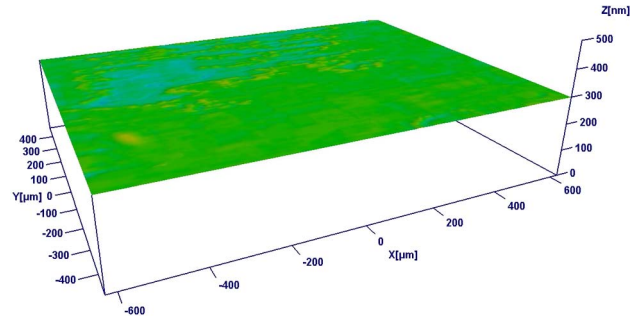

Fig. 25. (Color online) Estimated thickness profile of the region of the thickness standard that is nominally 300 nm in thickness, as obtained by GMFT-1 fitting.

$$a(B) = \alpha(B)a(R), \tag{10}$$

$$a(G) = \alpha(G)a(R), \tag{11}$$

where $\alpha(B)$ and $\alpha(G)$ are the ratios of the bias parameters. These ratios are determined primarily by the spectral characteristics of the illumination and the camera. Therefore, they are regarded as device parameters, and can be obtained through other GMFT fitting experiments.

Similarly, we assume that the ratios among the modulation parameters $b(j)$ are constant. Then, $b(B)$ and $b(G)$ are expressed as

$$b(B) = \beta(B)b(R), \tag{12}$$

$$b(G) = \beta(G)b(R), \tag{13}$$

where $\beta(B)$ and $\beta(G)$ are the ratios of the modulation parameters. These ratios are determined primarily by the optical properties of the target film structure, namely the refractive index dispersions of the film and the substrate. Therefore, they are regarded as sample parameters, and can be obtained through other GMFT fitting experiments for the same materials.

By these two assumptions, the unknown parameters are reduced to three—that is, $t(1)$, $a(R)$, and $b(R)$.
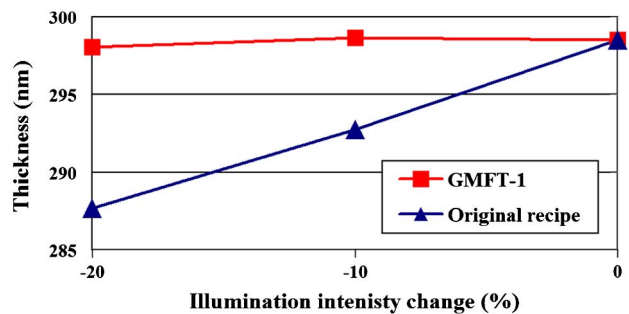

Fig. 26. (Color online) Relationship between the estimated thicknesses of the region that is nominally 300 nm in thickness and the illumination intensity obtained by using the original recipe and GMFT-1 algorithm.

Table 3. List of Modified GMFT Algorithms

Thickness	No. of Points	Name	Unknown Thicknesses	Unknown Parameters	Total Unknown Values	Observed Data	Known Data
Unknown	1	GMFT-1	$t(1)$	$a(3)$ $b(3)$	3	≥ 3	α, β
	2	GMFT-2	$t(1)$ $t(2)$	$a(1), \ldots, a(3)$ $b(3)$	6	≥ 6	β
	$n(\geq 3)$	GMFT	$t(1), \ldots, t(n)$	$a(1), \ldots, a(3)$ $b(1), \ldots, b(3)$	$n + 6$	$3n$	
Known	1	GMFT-1f	–	$a(1), \ldots, a(3)$	3	≥ 3	$t(1)$ $b(1), \ldots, b(3)$
	$n(\geq 2)$	GMFT-f	–	$a(1), \ldots, a(3)$ $b(1), \ldots, b(3)$	6	$3n$	$t(1), \ldots, t(n)$

D. Experiments

From Table 2, we obtained $\alpha(B) = 1.18$, $\alpha(G) = 1.07$, $\beta(B) = 1.02$, and $\beta(G) = 1.07$. Using these values, we estimated the thickness profile of the region of the thickness standard that is nominally 300 nm in thickness. The captured image is shown in Fig. 24, with the selected point used for GMFT-1 fitting. The result is shown in Fig. 25. The average was 299 nm, and the standard deviation was 0.42 nm rms.

E. Experimental Proof of Intensity Drift Compensation

Here, we show that the GMFT-1 algorithm can compensate the illumination intensity drift. From the color image shown in Fig. 24, we made two images with brightness decreased by 10% and 20%. For the three images, we estimated the thickness profile using two recipes: (1) the same recipe obtained for the original image, and (2) the new recalculated recipes based on the GMFT-1 algorithm. The result is shown in Fig. 26. The measurement dependence on the illumination intensity can be decreased considerably by adopting the modified algorithm.

6. Discussion

A. Thickness Measurement Resolution

In our previous study [11], we made a theoretical analysis of the measurement resolution of the GMF method. The result suggests that we can expect approximately 1 nm optical thickness resolution in the case of an 8 bit intensity scale, provided that the noise level of the observed intensity is within a few gray levels. With a 10 bit intensity scale, subnanometer resolution could be achieved.

B. Maximum Measurable Thickness

In the GMFT method, there is theoretically no limit to the thickness range. We note that the estimated thickness is dependent on the initial estimate of the thickness, as discussed above.

The issue of the maximum measurable thickness of the ACOS method is almost the same as that with three-wavelength spatial carrier interferometry [12], because the thickness is determined by spectral unwrapping using the phases of three wavelengths. The unambiguous range depends on various factors, including wavelengths, electronic noise, and optical errors. As for the wavelengths, the 470/560/600 nm combination used in this paper was selected by Kitagawa [12] as the optimum one that provides an unambiguous range of approximately 4 μm. Therefore, a measurement range of at least 4 μm can be expected.

C. Further Modifications of the GMFT Algorithm

In Subsection 5.B, we introduced the GMFT-1 algorithm for the almost-uniform thickness target. Similarly we can obtain modified GMFT algorithms for various cases as shown in Table 3. For example, the GMFT-2 algorithm is used when the target has two thickness areas. GMFT-1f is used when there is a single point with known thickness.

7. Conclusion

We have proposed a new interferometric thickness profiling technique, the GMFT method, which enables us to measure the thickness distribution from a single color image captured by a CCD camera. It is based on a model-fitting algorithm and estimates the model parameters and the thicknesses of several points simultaneously from their multiwavelength intensity data.

A necessary condition for obtaining the solution is that there are at least three points of different thicknesses in the case of three wavelengths. When three points are selected for the fitting, a total of

nine unknown parameters (e.g., three thicknesses and six waveform parameters) are estimated by least-squares fitting. Once the waveform parameters are estimated by this technique, they can be used for thickness estimation of all points except fitted points, which can be executed by a much simpler and faster algorithm using the arccosine function. Furthermore, we have developed modified GMFT algorithms for the cases in which the necessary condition cannot be satisfied. The proposed method has been validated by computer simulations and experiments.

The most significant feature of this technique is that no preliminary calibration is required. That is, if there are at least three points of different thicknesses in the test sample, a type of self-calibration is achieved. Other advantages include (1) high-speed 2D measurement, (2) wide measurement range, and (3) low cost and simple optics.

References

1. T. S. Hyvarinen, E. Herrala, and A. Dall'Ava, "Direct sight imaging spectrograph: a unique add-on component brings spectral imaging to industrial applications," Proc. SPIE **3302**, 165–175 (1998).
2. M. Ohlidal, V. Cudek, I. Ohlidal, and P. Klapetek, "Optical characterization of non-uniform thin films using imaging spectrophotometry," Proc. SPIE **5963**, 596329 (2005).
3. G. Jin, R. Jansson, and H. Arwin, "Imaging ellipsometry revisited: developments for visualization of thin transparent layers on silicon substrates," Rev. Sci. Instrum. **67**, 2930–2936 (1996).
4. T. Sato, T. Araki, Y. Sasaki, T. Tsuru, T. Tadokoro, and S. Kawakami, "Compact ellipsometer employing a static polarimeter module with arrayed polarizer and wave-plate elements," Appl. Opt. **46**, 4963–4967 (2007).
5. S. Parthasarathy, D. Wolfe, E. Hu, S. Hackwood, and G. Beni, "A color vision system for film thickness determination," in *Proceedings of IEEE Conference on Robotics and Automation* (IEEE, 1987), pp. 515–519.
6. D. Birnie, "Optical video interpretation of interference colors from thin transparent films on silicon," Mater. Lett. **58**, 2795–2800 (2004).
7. M. Kubo, Y. Ohtsubo, N. Kawashima, and H. Marumo, "Head slider flying height measurement using a color image processing technique," JSME Int. J. **32**, 264–268 (1989).
8. M. Hartl, I. Krupka, R. Poliscuk, and M. Liska, "Computer-aided evaluation of chromatic interferograms," presented at *Fifth International Conference in Central Europe on Computer Graphics and Visualization*, Plzeň, Czech Republic, 10–14 February 1997, pp. 45–54.
9. M. Eguchi and T. Yamamoto, "Film thickness measurement using white light spacer interferometry and its calibration by HSV color space," presented at *5th International Conference on Tribology*, Parma, Italy, 20–22 September 2006.
10. K. Kitagawa, "Multi-wavelength single-shot interferometry without carrier fringe introduction," Proc. SPIE **8000**, 800009 (2011).
11. K. Kitagawa, "Single-shot surface profiling by multi-wavelength interferometry without carrier fringe introduction," J. Electron. Imaging **21**, 021107 (2012).
12. K. Kitagawa, "Fast surface profiling by multi-wavelength single-shot interferometry," Int. J. Optomechatronics **4**, 136–156 (2010).
13. R. Fletcher and M. J. D. Powell, "A rapidly convergent descent method for minimization," Comput. J. **6**, 163–168 (1963).
14. C. Tilford, "Analytical procedure for determining lengths from fractional fringes," Appl. Opt. **16**, 1857–1860 (1977).